

## Supporting Information

# **Highly Efficient and Durable P, Ru-CeO<sub>2</sub> Self-supporting Electrodes Toward Industrial-level Hydrogen Production**

Wenguang Ma, Xiaodong Yang, Yanru Xu, Cuncheng Li\*, Yiqiang Sun\*, Qi Shen\*, Zhixin Sun\*

Dr. W. G. Ma, Dr. X. D. Yang, Dr. Y. R. Xu, Prof. C. C. Li, Prof. Y. Q. Sun, Prof. Q. Shen

School of Chemistry and Chemical Engineering, University of Jinan, Jinan, 250055, P. R. China

Dr. Z. X. Sun  
Shandong University of Traditional Chinese Medicine

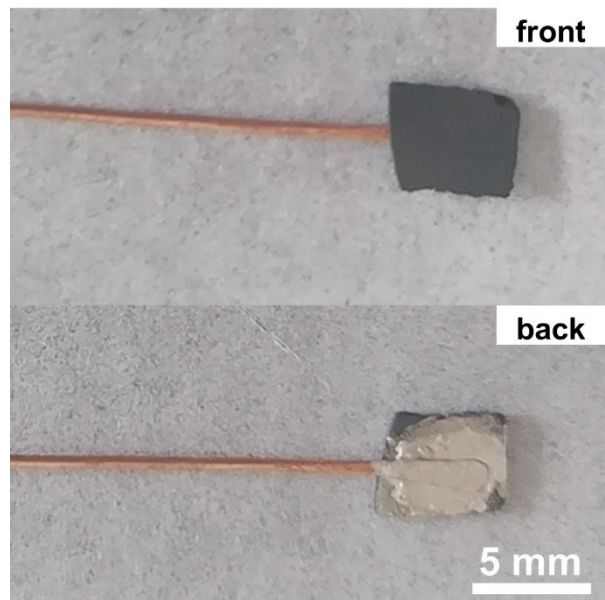


**Figure S1.** The optical photo of the P, Ru-CeO<sub>2</sub> self-supporting electrode.

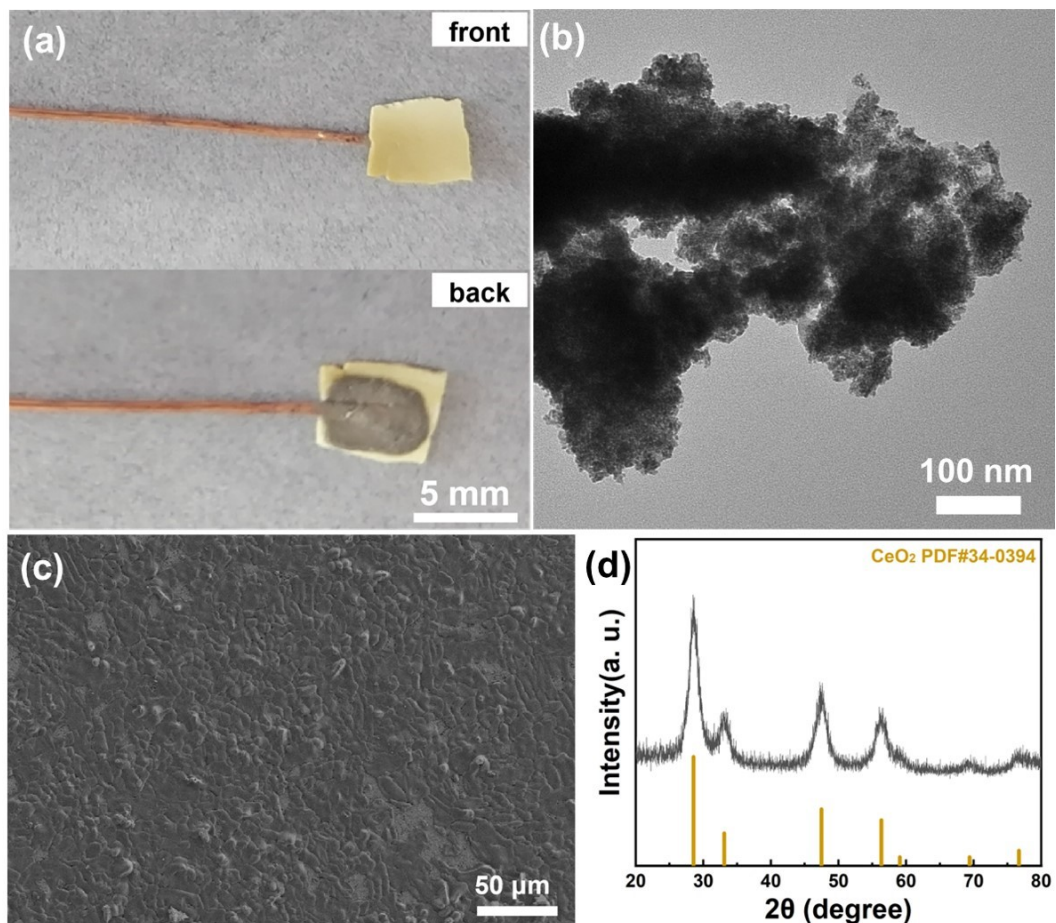


**Figure S2.** (a) Optical photo, (b) TEM image, (c) SEM image and (d) XRD pattern of the pristine CeO<sub>2</sub> self-supporting electrode.

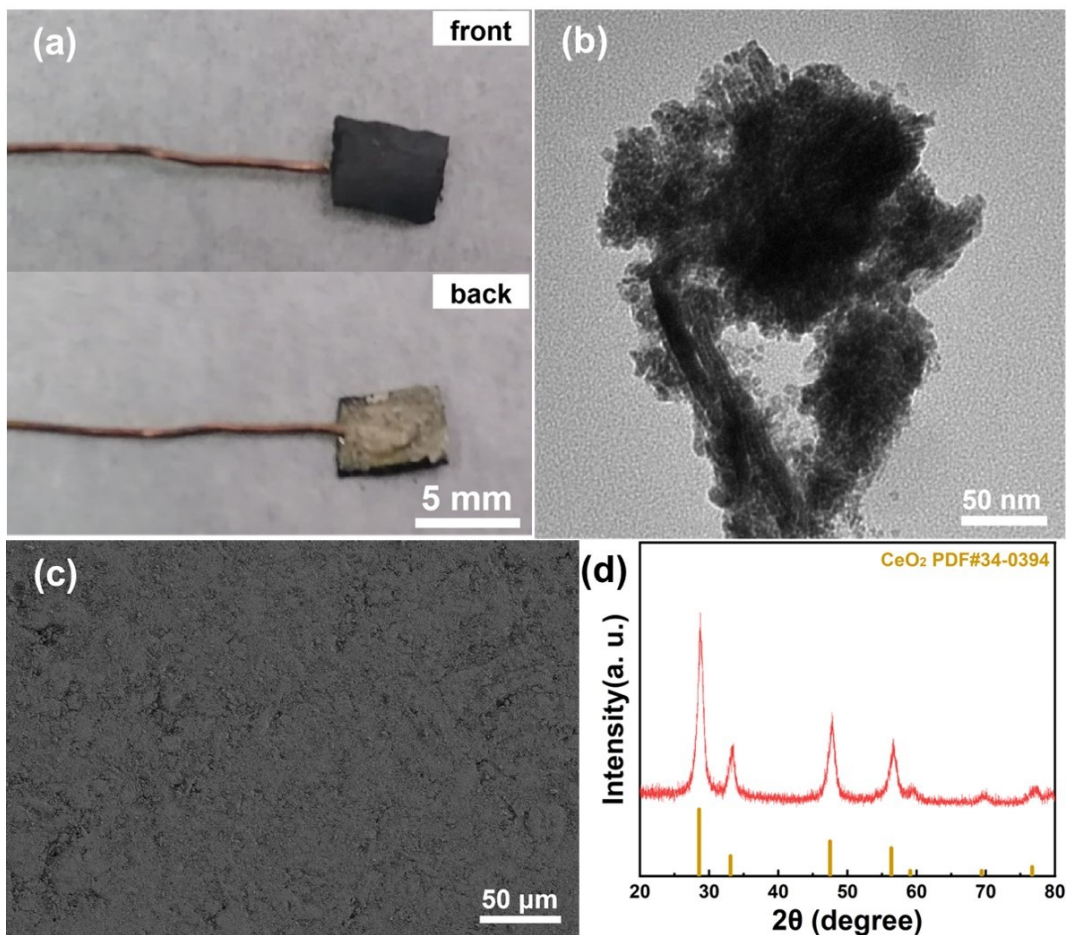


**Figure S3.** (a) Optical photo, (b) TEM image, (c) TEM image and (d) XRD pattern of the Ru-CeO<sub>2</sub> self-supporting electrode.

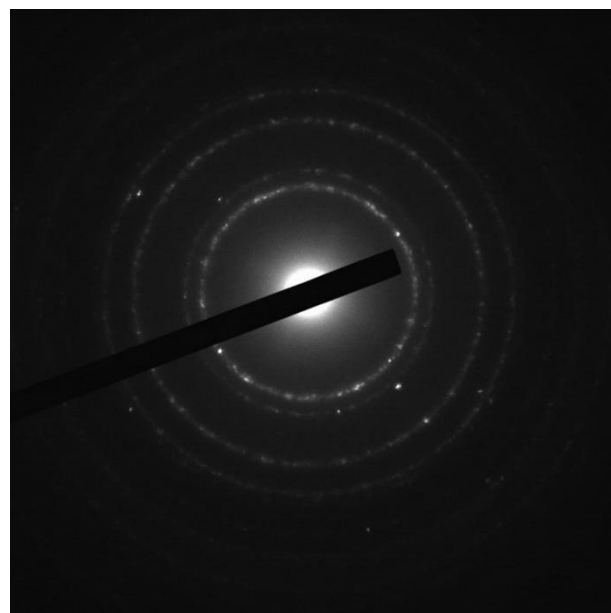


**Figure S4.** SAED pattern of the P, Ru-CeO<sub>2</sub> catalyst.

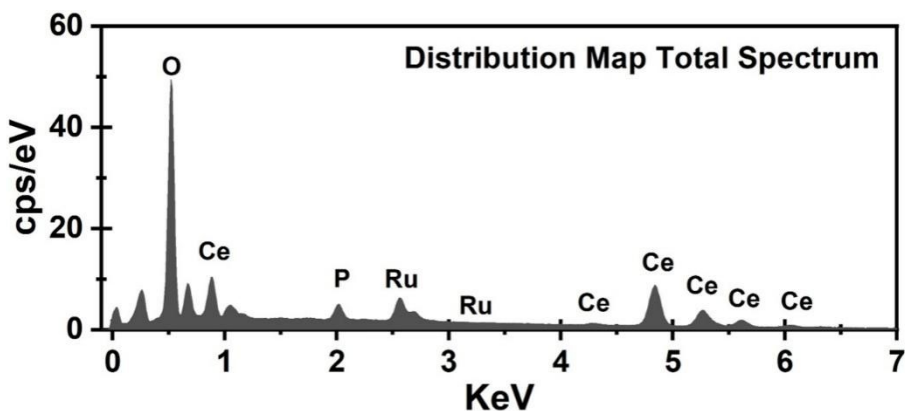


**Figure S5.** EDX spectrum of the P, Ru-CeO<sub>2</sub> self-supporting electrode.

Distribution Map Total Spectrum				
element	Line Type	Weight%	wt% Sigma	Atomic%
O	K	17.03	0.10	54.05
P	K	1.48	0.03	2.49
Ru	L	6.66	0.10	3.43
Ce	M	71.57	0.18	26.62
Other	-	3.26	-	13.41
<b>total</b>	<b>-</b>	<b>100</b>	<b>-</b>	<b>100</b>

**Table S1.** Relative proportions of main elements, corresponding to Figure S5.

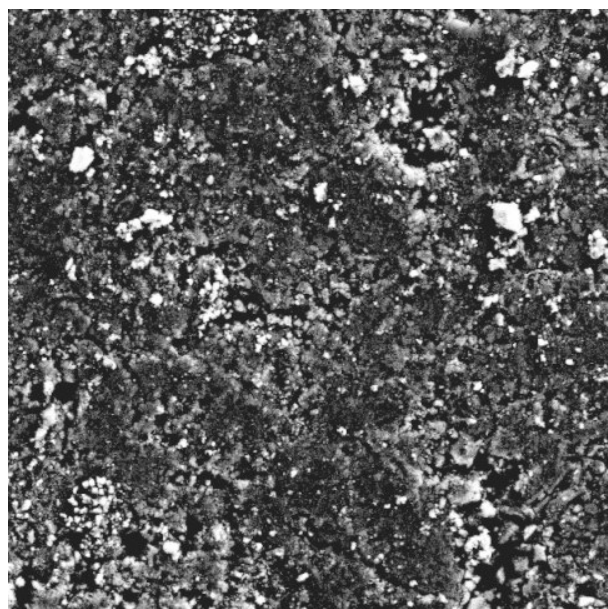


**Figure S6.** The SEM image for elemental mapping of the P, Ru-CeO<sub>2</sub> self-supporting electrode.

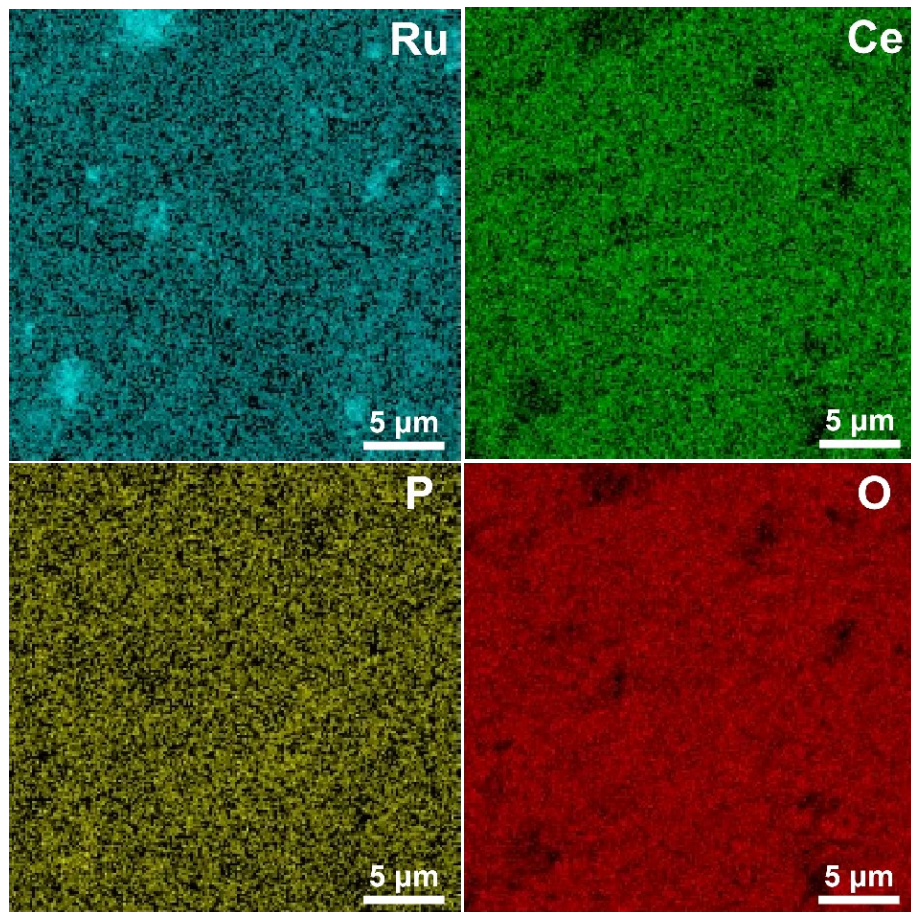


**Figure S7.** The corresponding elemental mapping image in Figure S5 of the P, Ru-CeO<sub>2</sub> self-supporting electrode.

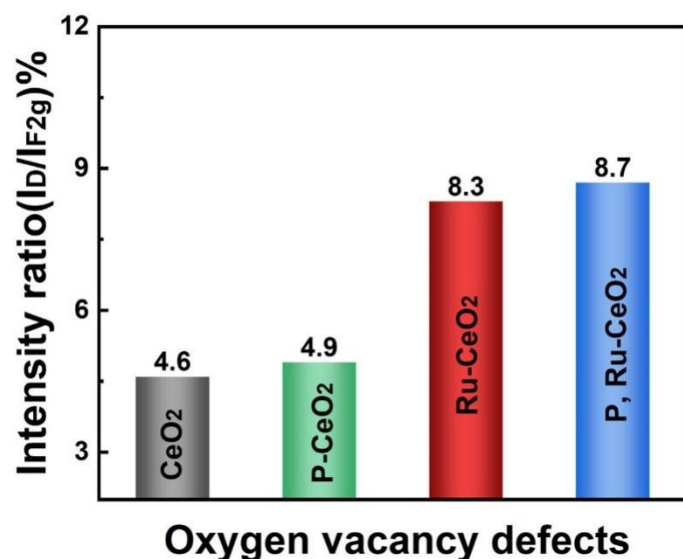


**Figure S8.** Peak intensity ratio of  $I_D/I_{F2g}$  over CeO<sub>2</sub>, P-CeO<sub>2</sub>, Ru-CeO<sub>2</sub> and P, Ru-CeO<sub>2</sub> catalysts.

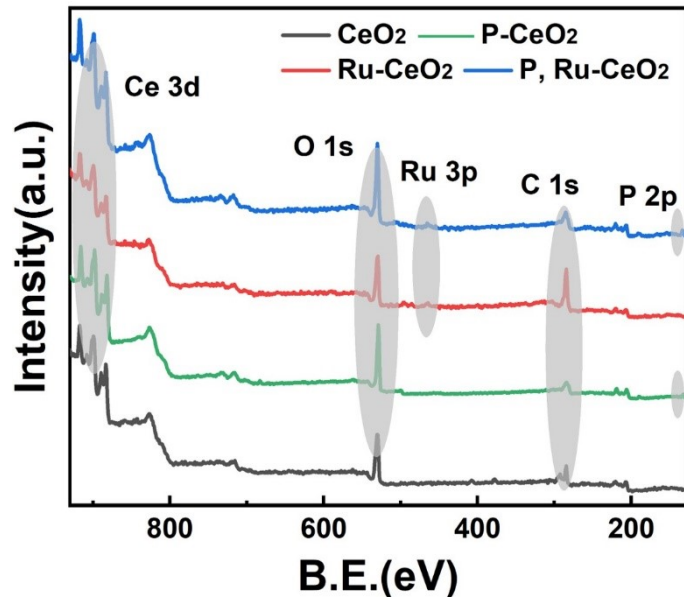


**Figure S9.** XPS survey scan spectrum of the pristine CeO<sub>2</sub>, P-CeO<sub>2</sub>, Ru-CeO<sub>2</sub> and P, Ru-CeO<sub>2</sub> catalysts.

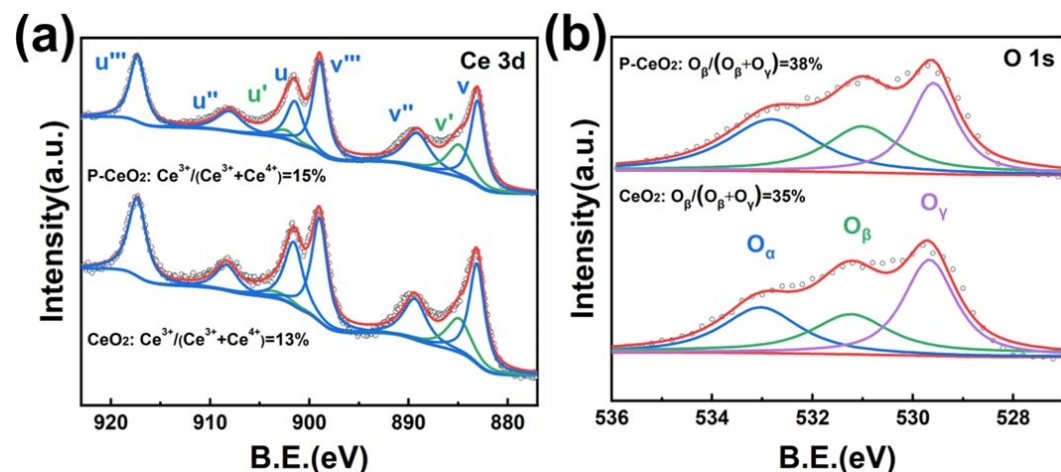


**Figure S10.** XPS of the pristine CeO<sub>2</sub>, P-CeO<sub>2</sub> catalysts: (a) Ce 3d orbitals, (b) O 1s orbitals.

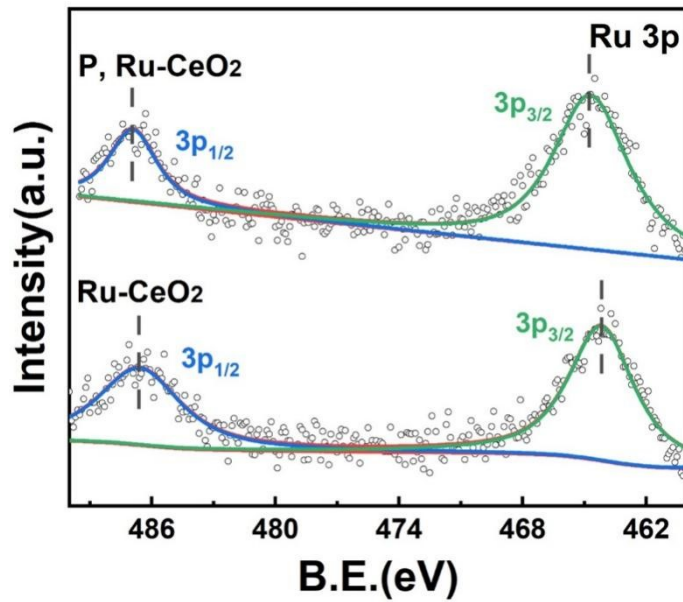


**Figure S11.** XPS of Ru-CeO<sub>2</sub> and P, Ru-CeO<sub>2</sub> catalysts: Ru 3p orbitals.

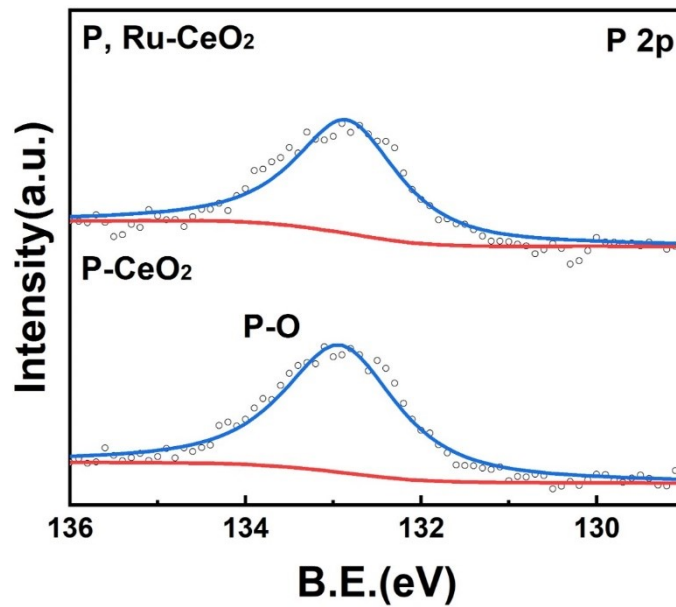


**Figure S12.** XPS of P-CeO<sub>2</sub> and P, Ru-CeO<sub>2</sub> catalysts: P 2p orbitals.

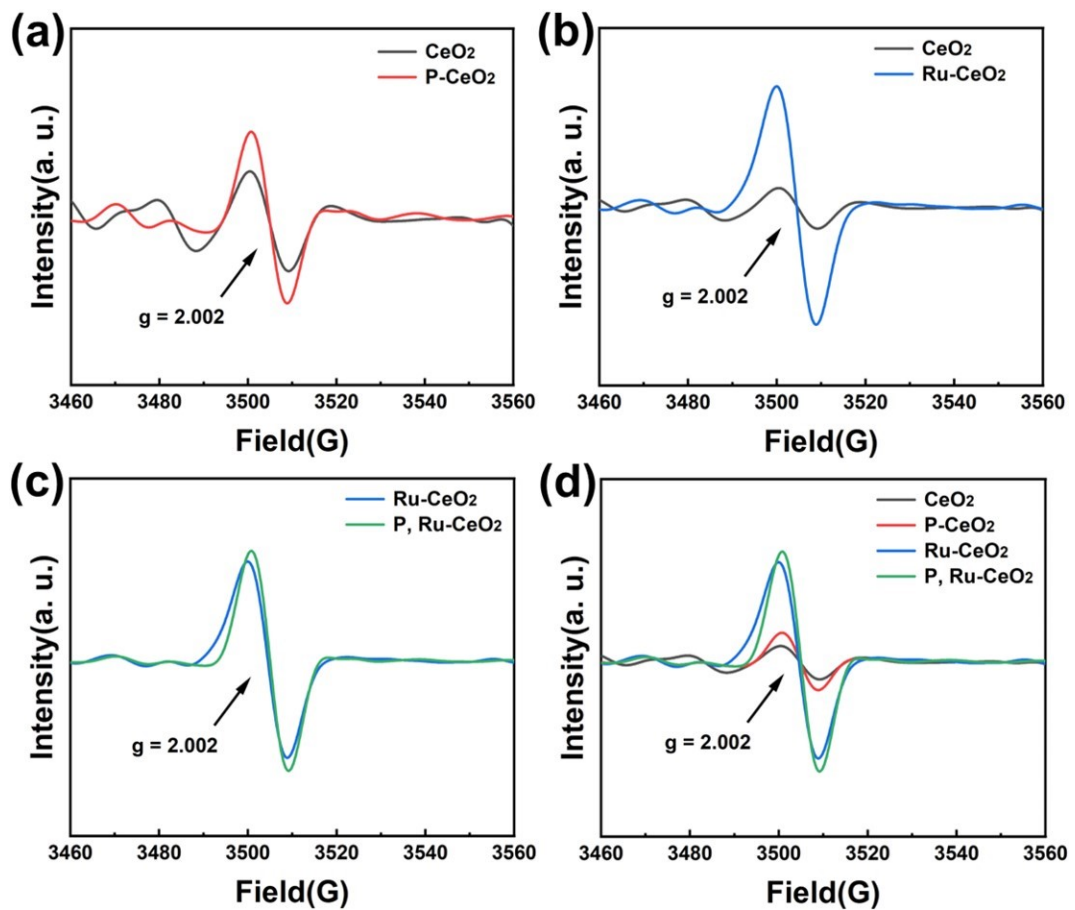


**Figure S13.** EPR spectrum of the catalysts: (a)  $\text{CeO}_2$  and  $\text{P}-\text{CeO}_2$ , (b)  $\text{CeO}_2$  and  $\text{Ru}-\text{CeO}_2$ , (c)  $\text{Ru}-\text{CeO}_2$  and  $\text{P}, \text{Ru}-\text{CeO}_2$ , (d)  $\text{CeO}_2$ ,  $\text{P}-\text{CeO}_2$ ,  $\text{Ru}-\text{CeO}_2$  and  $\text{P}, \text{Ru}-\text{CeO}_2$ .

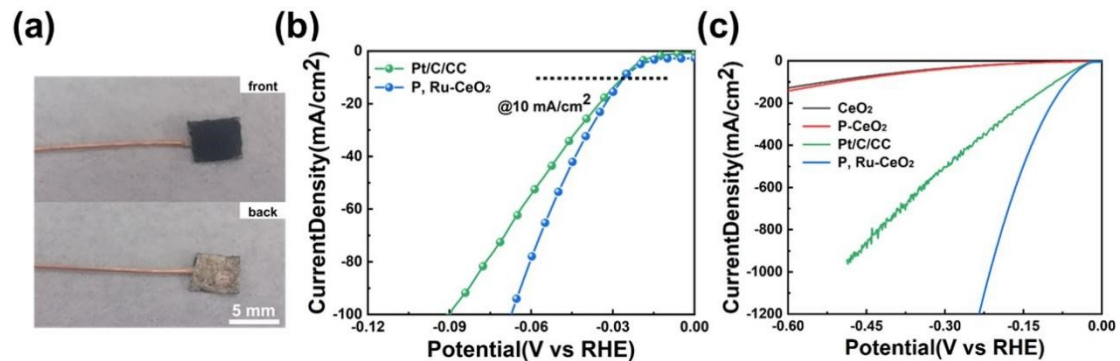


**Figure S14.** (a) Commercial Pt/C working electrode loaded on CC. iR-corrected polarization curves of the pure  $\text{CeO}_2$ ,  $\text{P}-\text{CeO}_2$ ,  $\text{P}, \text{Ru}-\text{CeO}_2$  self-supporting working electrodes and commercial Pt/C/CC: (b) @low-current density; (c) @high-current density.

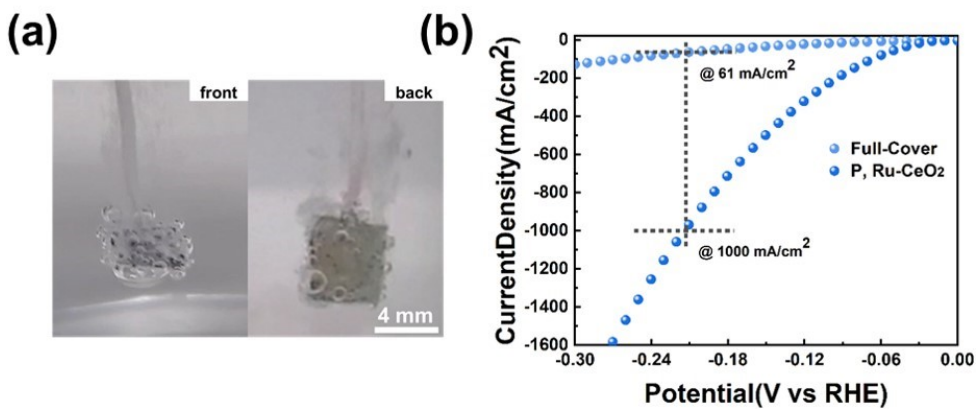


**Figure S15.** (a) the comparison between the front and back of the P, Ru-CeO<sub>2</sub> self-supporting working electrode. (b) iR-corrected polarization curves of the Full-Cover-P, Ru-CeO<sub>2</sub>, P, Ru-CeO<sub>2</sub> self-supporting working electrodes.

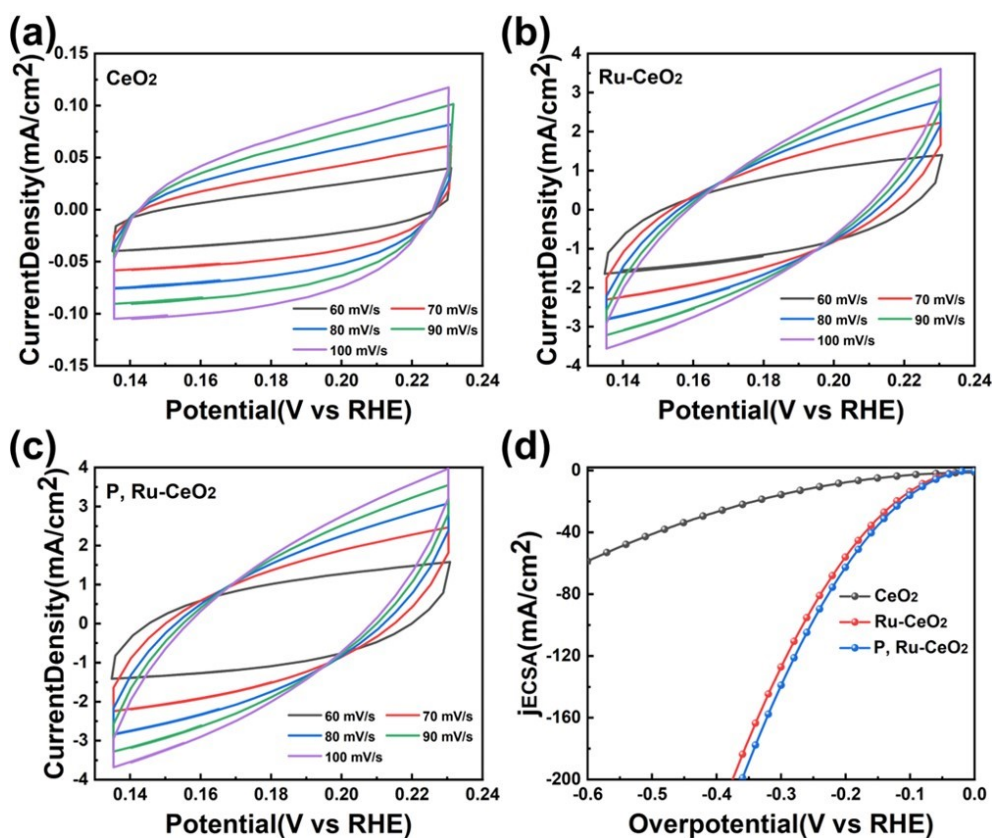


**Figure S16.** Electrochemical double-layer capacitance measurements at different scan rates for HER. Cyclic voltammograms of (a) pure CeO<sub>2</sub>, (b) Ru-CeO<sub>2</sub> and (c) P, Ru-CeO<sub>2</sub> self-supporting working electrodes. (d) HER polarization curves normalized by the electrochemical double-layer capacitance.

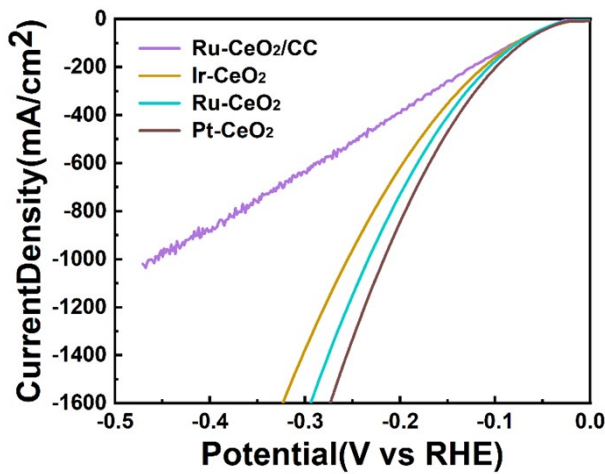


**Figure S17.** iR-corrected polarization curves of the Ir-CeO<sub>2</sub>, Ru-CeO<sub>2</sub>, Pt-CeO<sub>2</sub> self-supporting working electrodes, and the Ru-CeO<sub>2</sub>/CC.

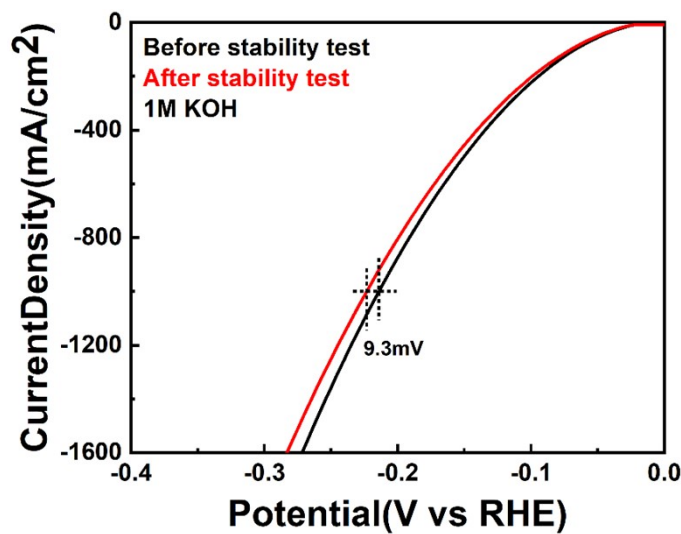


**Figure S18.** iR-corrected polarization curves of the P, Ru-CeO<sub>2</sub> self-supporting electrode before and after 5000 CV cycles in 1 M KOH.

materials	$\eta_{HER}(mV)$	Tafel(mV/dec)	Reference
This work	215	25	—
Pt/TiO <sub>2</sub> /Ni(OH) <sub>2</sub> /NF	227	39	Ref.1 <sup>1</sup>
NiCo@RuO <sub>2</sub> HNAs/NF	236	69	Ref.2 <sup>2</sup>
FeNiZn/FeNi <sub>3</sub> @NiFe	245	45	Ref.3 <sup>3</sup>
Ru-CoO <sub>x</sub> /NF	252	28	Ref.4 <sup>4</sup>
Ni-W <sub>2</sub> N@NF	276	46	Ref.5 <sup>5</sup>
Sr <sub>2</sub> RuO <sub>4</sub> bulk SC	278	26	Ref.6 <sup>6</sup>
Co-SA/CC	294	97	Ref.7 <sup>7</sup>
Ni-Co-P/CFP	295	31	Ref.8 <sup>8</sup>
Self-Standing Pt NC/CF	331	61	Ref.9 <sup>9</sup>
Cu <sub>3</sub> P-FeP@CC	338	84	Ref.10 <sup>10</sup>

**Table S2.** Comparison of the HER performance of the P, Ru-CeO<sub>2</sub> self-supporting working electrode with the similar catalysts at 1000 mA·cm<sup>-2</sup> in 1.0 M KOH.

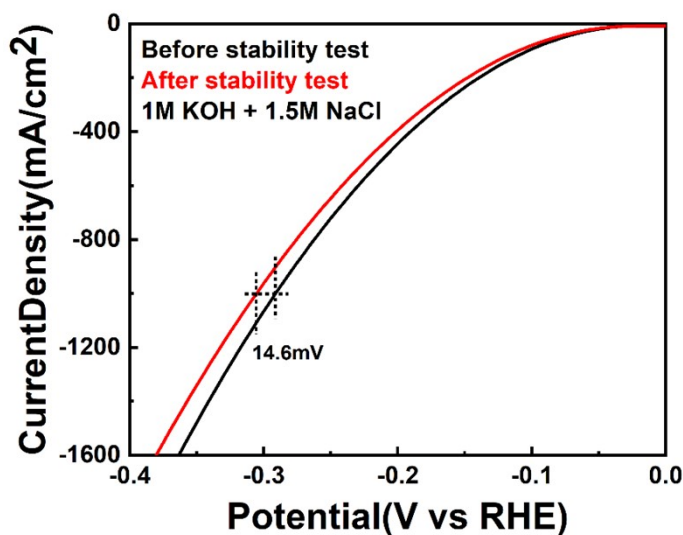


**Figure S19.** iR-corrected polarization curves of the P, Ru-CeO<sub>2</sub> self-supporting electrode before and after 5000 CV cycles in 1 M KOH+1.5 M NaCl.

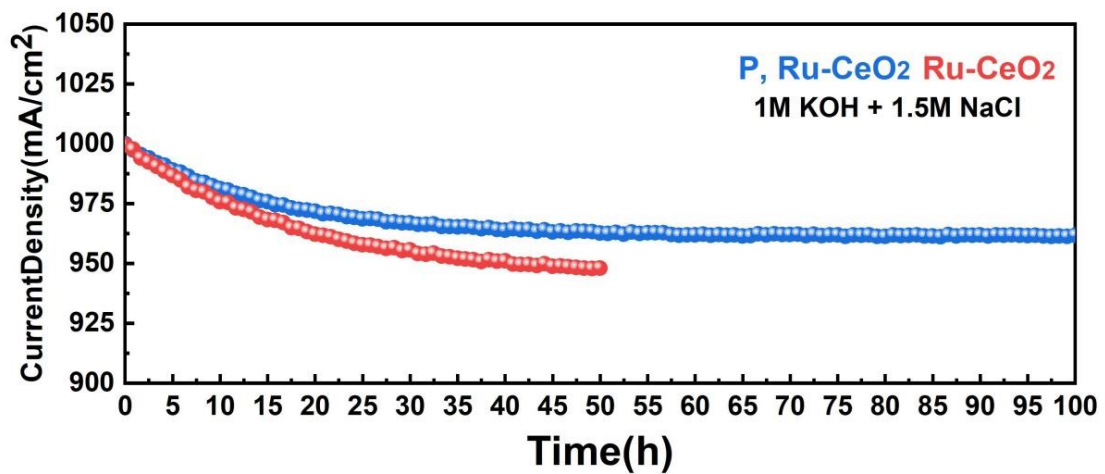


**Figure S20.** Chronoamperometric curves of the Ru-CeO<sub>2</sub> self-supporting electrodes and the P, Ru-CeO<sub>2</sub> self-supporting electrodes.

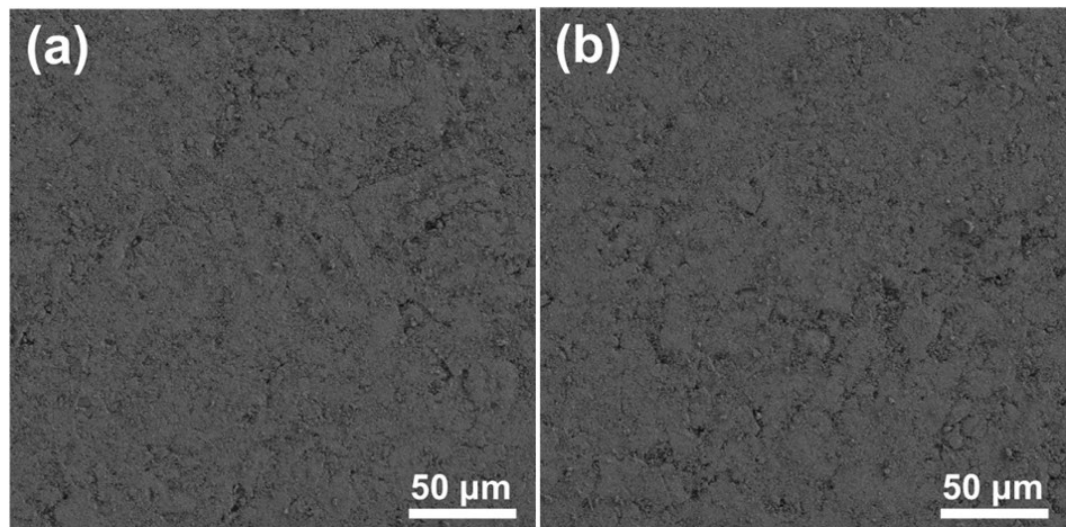


**Figure S21.** SEM images of the P, Ru-CeO<sub>2</sub> self-supporting electrode (a) before and (b) after durability test in 1 M KOH+1.5 M NaCl.

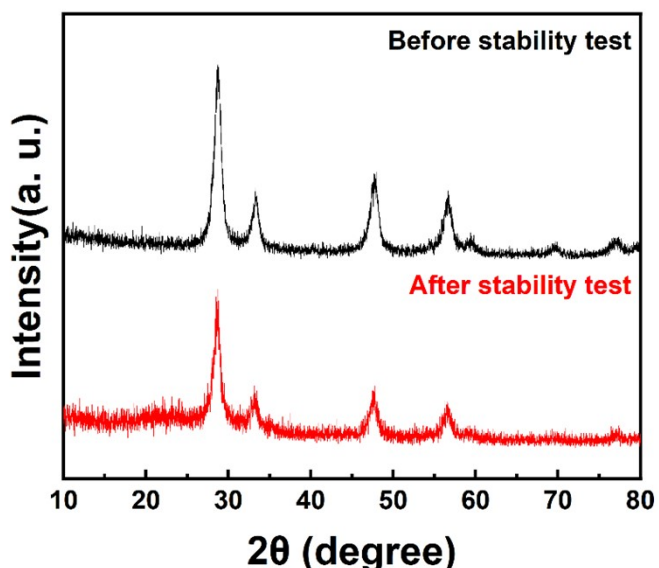


**Figure S22.** XRD pattern of the P, Ru-CeO<sub>2</sub> catalyst after durability test in 1 M KOH+1.5 M NaCl.

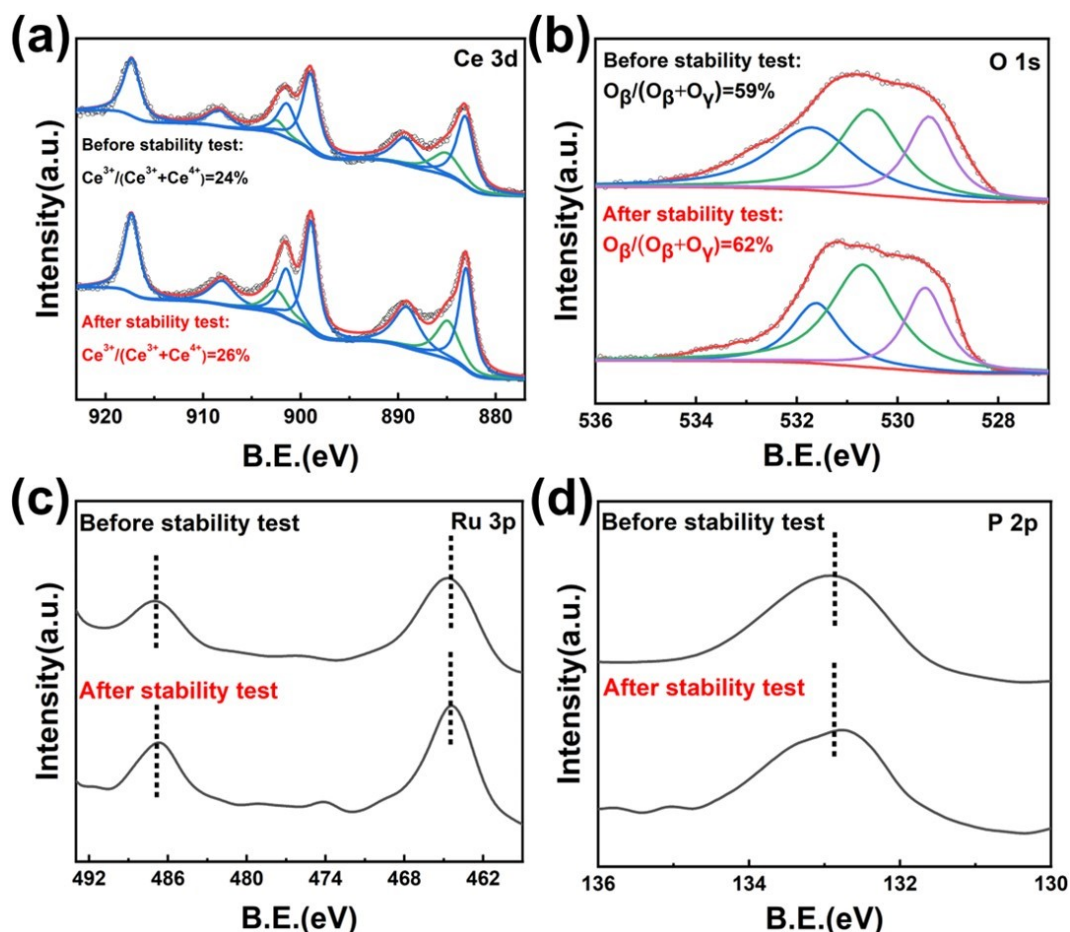


**Figure S23.** XPS of the P, Ru-CeO<sub>2</sub> catalyst after durability test in 1 M KOH+1.5 M NaCl. (a) Ce 3d. (b) O 1s. (c) Ru 3p. (d) P 2p.

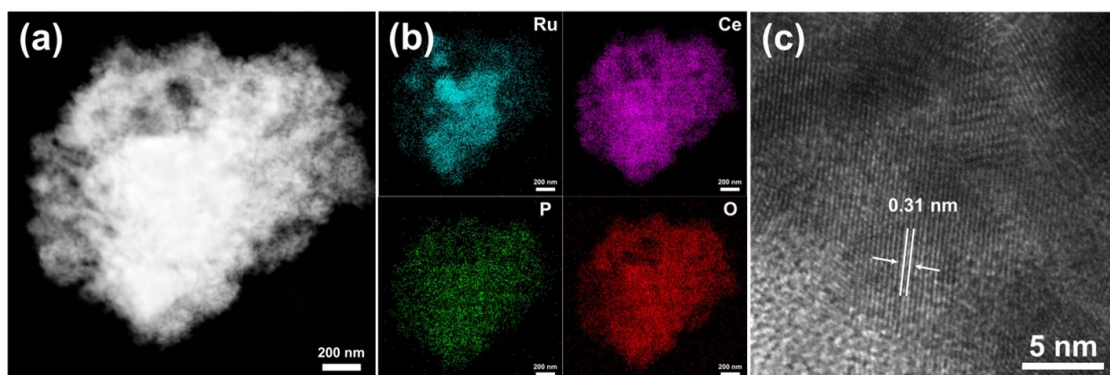


**Figure S24.** TEM images of the P, Ru-CeO<sub>2</sub> catalyst after durability test in 1 M KOH+1.5 M NaCl. (a) HADDF-STEM. (b) EDS. (c) HRTEM.

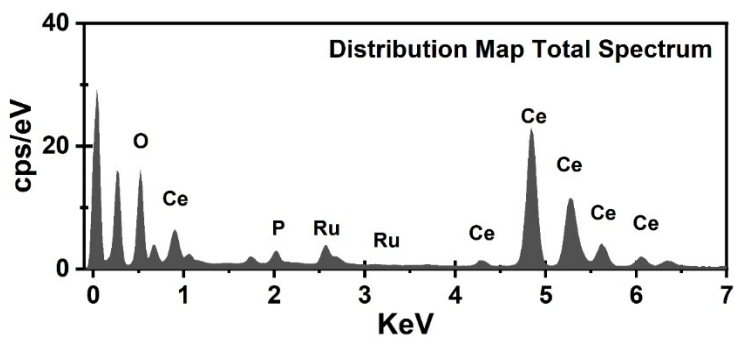


**Figure S25.** EDX spectrum of the P, Ru-CeO<sub>2</sub> catalyst, corresponding to **Figure S24**.

Distribution Map Total Spectrum			
element	Line Type	Weight%	$\sigma$
Ce	M	72.48	0.2
O	K	17.57	0.1
Ru	L	6.12	0.2
P	K	1.61	0.1
Other	-	2.22	-
<b>total</b>	<b>-</b>	<b>100</b>	<b>-</b>

**Table S3.** Relative proportions of main elements, corresponding to **Figure S25**.

## References

- 1 A. Kong, M. Peng, M. Liu, Y. Lv, H. Zhang, Y. Gao, J. Liu, Y. Fu, W. Li and J. Zhang, *Applied Catalysis B-Environmental*, 2022, **316**, 121654.
- 2 H. Yi, X. Zhang, Z. Ai, S. Song and Q. An, *ChemSusChem*, 2022, **15**, 2201532.

- 3 Q. Zhou, C. Xu, J. Hou, W. Ma, T. Jian, S. Yan and H. Liu, *Nano-Micro Letters*, 2023, **15**, 95.
- 4 D. Wu, D. Chen, J. Zhu and S. Mu, *Small*, 2021, **17**, 2102777.
- 5 Z. Dan, W. Liang, X. Gong, X. Lin, W. Zhang, Z. Le, F. Xie, J. Chen, M. Yang, N. Wang, Y. Jin and H. Meng, *ACS Materials Letters*, 2022, **4**, 1374-1380.
- 6 Y. Zhang, K. E. Arpino, Q. Yang, N. Kikugawa, D. A. Sokolov, C. W. Hicks, J. Liu, C. Felser and G. Li, *Nature Communications*, 2022, **13**, 7784.
- 7 P. Zhao, C. Peng, Q. Zhang, X. Fan, H. Chen, Y. Zhu and Y. Min, *Chemical Engineering Journal*, 2023, **461**, 142037.
- 8 X. Chen, X. Zhao, Y. Wang, S. Wang, Y. Shang, J. Xu, F. Guo and Y. Zhang, *ChemCatChem*, 2021, **13**, 3619-3627.
- 9 Y. Tan, R. Xie, S. Zhao, X. Lu, L. Liu, F. Zhao, C. Li, H. Jiang, G. Chai, D. J. L. Brett, P. R. Shearing, G. He and I. P. Parkin, *Advanced Functional Materials*, 2021, **31**, 2105579.
- 10 C. Chai, J. Yang, C. Jiang, L. Liu and J. Xi, *Acs Applied Energy Materials*, 2022, **5**, 2909-2917.